Helicopter Flight Procedures for Community Noise Reduction

Eric Greenwood
Aeroacoustics Branch
NASA Langley Research Center
Hampton, VA

ABSTRACT

A computationally efficient, semiempirical noise model suitable for maneuvering flight noise prediction is used to evaluate the community noise impact of practical variations on several helicopter flight procedures typical of normal operations. Turns, "quick-stops," approaches, climbs, and combinations of these maneuvers are assessed. Relatively small variations in flight procedures are shown to cause significant changes to Sound Exposure Levels over a wide area. Guidelines are developed for helicopter pilots intended to provide effective strategies for reducing the negative effects of helicopter noise on the community. Finally, direct optimization of flight trajectories is conducted to identify low noise optimal flight procedures and quantify the magnitude of community noise reductions that can be obtained through tailored helicopter flight procedures. Physically realizable optimal turns and approaches are identified that achieve global noise reductions of as much as 10 dBA Sound Exposure Level.

INTRODUCTION

Helicopters serve a number of useful roles within the community, such as electronic news gathering and aerial photography, inspection and maintenance of power lines, police and emergency medical services, aerial cranes, cropdusting, civil transport, and sightseeing. However, community acceptance of these operations is limited by the resulting noise. For instance, voluntary restrictions on helicopter operations have recently been adopted in the Los Angeles and New York City areas to increase community acceptance (Refs. 1–3). The acoustic impact of civil helicopter operations will need to be reduced in order to allow for a greater variety and volume of helicopter operations in the future. In the long term, design changes such as reduced tip speeds or the widespread adoption of active and passive rotor noise reduction technologies may result in significant reductions in the noise emitted by future helicopters. However, because the noise radiated by helicopters is extremely sensitive to the helicopter's operating state, immediate noise reductions can be achieved through the development of low noise flight procedures applicable to the existing civil fleet.

Previous work on developing low noise helicopter flight procedures has focused on the approach phase (Ref. 4). As the helicopter descends, the tip vortices trailed from the leading edge of the rotor disk convect through the rotor tip-path-plane resulting in high levels of Blade-Vortex Interaction (BVI) noise. Depending on the airspeed, drag, weight, and disk loading of the helicopter, BVI noise reaches a maximum at a specific descent rate during steady flight. This phenomenon has been exploited to generate two-dimensional approach profiles from nominally steady-flight segments that are intended to avoid high noise flight states when the helicopter is in noise-sensitive areas close to the ground (Ref. 5). In practice, approach profiles that do not consider the acoustic effects of nonsteady flight do not result in minimum noise approach trajectories. For instance, longitudinal acceleration or deceleration change the flight path angles where BVI occur, reducing the effectiveness of approach profiles developed using steady-flight modeling (Ref. 6). However, this effect can be exploited to cause reductions in BVI noise (Ref. 7), e.g., by accelerating along a shallow approach trajectory to "push" the rotor wake further below the rotor and decrease BVI noise.

Over the last decade, considerable research has been conducted in order to incorporate nonsteady maneuvering flight effects into helicopter noise models with the aim of developing effective low noise flight procedures. The Quasi-Static Acoustic Mapping (Q-SAM) approach was developed (Ref. 8) and experimentally verified (Ref. 9) to draw equivalences between steady-state and constant longitudinal accelerating flight conditions. This method allows two-dimensional segmented approach profiles to be developed that use the effects of longitudinal acceleration to achieve further noise reductions (Ref. 10). However, because BVI noise is minimal at both high descent rate / high deceleration and low descent rate / high acceleration flight conditions, the "optimal" low noise approach profile produced with the segmented trajectory model is an unrealistic "bang-bang" solution, i.e., the simulated helicopter instantly—and unrealistically—transitions between steep and shallow flight path angle segments to avoid BVI noise (Ref. 10). The behavior can be limited by imposing additional artificial constraints to the optimization (Refs. 11, 12), but still fails to account for the acoustic impact of transitions between the straight line segments. Moreover, the longitudinal Q-SAM equivalence cannot accurately account for the changes in noise caused by lateral maneuvers, including steady turning flight (Ref. 13), limiting applicability of the model to two-dimensional approach profiles.

The objective of this paper is to apply a model of helicopter

Presented at the American Helicopter Society 73rd Annual Forum, Fort Worth, TX, May 2017.

noise that can accurately simulate the noise radiated over continuous three-dimensional maneuvering flight trajectories in order to

- develop practical guidance on flight procedures for helicopter pilots that reduce community noise exposure;
- demonstrate the reductions in community noise levels that are possible through the development of low noise optimal flight procedures.

APPROACH

The Fundamental Rotorcraft Acoustic Modeling from Experiments (FRAME) technique, developed by the author, constructs nondimensional aeroacoustic models of rotor noise radiation by fitting a nondimensional aeroacoustic model to measured acoustic data from both wind tunnel and flight experiments. Because a computational model of the major rotor harmonic noise sources is constructed, noise estimates can be obtained at flight conditions and radiation directions that were not originally measured (Refs. 14,15). The FRAME model was later extended to maneuvering flight conditions by introducing a dynamic prescribed wake model for BVI noise (Ref. 16). The model showed good agreement with measured data for several transient maneuvers and could be run in real time for a single observer; however, the generation of ground noise contours for assessing the community noise impact of helicopter flight procedures typically requires noise calculations for hundreds to thousands of observers–far too many for the model to be practically applied in the design and evaluation of low noise mission profiles. To provide a practical noise model for use in planning helicopter operations, the hybrid FRAME-QS model (Ref. 17) was developed. The FRAME-QS model combines the FRAME method of generalizing measured acoustic data to other operating conditions using physics-based modeling with an extension of the Q-SAM equivalence to three-dimensional flight over a continuous maneuvering flight trajectory.

The nondimensional FRAME model is first calibrated to a set of measured steady-flight data for a particular helicopter. The calibrated model is then used to generate an extensive database of spherical representations of the steady-state harmonic noise radiation of the helicopter at different advance ratios, tip Mach numbers, wake skew angles, and thrust coefficients. Both the main and tail rotor are included in the model; the tail rotor operating condition is assumed to track with changes in the main rotor operating condition. Later, waypoints can be entered for a proposed helicopter trajectory. A quintic interpolating spline is used to convert the waypoints into a high resolution trajectory. Using quintic splines guarantees a smooth variation in the velocity and acceleration from which the operating state of the helicopter can be derived for each moment in time using a simple point-mass dynamics model. Using the extended Q-SAM equivalence developed in Reference 17, the appropriate sphere is selected from the precomputed database and oriented with the predicted tip-path-plane orientations of the helicopter main and tail rotors at each instance in time. The FRAME-QS model, being quasi-static, does not consider the hysteresis of the wake; however, previous research has indicated that the dynamic distortion of the wake has little effect on noise radiation (Ref. 18) and accounts for perhaps a 1 dBA difference between advancing side and retreating side maneuvers (Ref. 13). Finally, the noise levels from the surface of the sphere are interpolated and propagated to a set of observers on the ground. By precalculating the FRAME noise data, ground noise contours can be computed rapidly and iterated upon to develop low noise procedures for various maneuvers. This approach was validated against experimental maneuvering flight noise data collected by NASA and Bell Helicopter for the Bell 430 in 2011 (Ref. 19) and was shown to capture the effects of maneuvering flight on helicopter noise radiation with good accuracy. For example, Figure 1 plots a comparison of predicted A-weighted Sound Pressure Level (SPL) to measured data at a microphone location ahead of the helicopter for the Bell 430 executing a both a fast pitch up maneuver (Figure 1a) and a roll-in to an advancing side turn (Figure 1b). In both cases, the FRAME-QS model provides excellent agreement with the measured data compared to predictions with a conventional segmented source noise model, accurately predicting the large increase in A-weighted noise levels caused by the increase in BVI due to the transient maneuver. The conventional segemented model underpredicts the SPL by as much as 10 dBA.

In this paper, the straight-ray propagation model used with FRAME-QS model is simplified to further decrease the computational time required to evaluate each maneuver. When the FRAME sphere database is constructed, the predicted pressure time history at each emission angle is converted to a frequency-domain power spectrum. From this spectrum, the A-weighting curve is applied to each main and tail rotor harmonic; the A-weighted SPL can then be computed on the sphere surface by summing the energy in each of these weighted harmonics. Additionally, an excess atmospheric attenuation factor can be computed for each A-weighted SPL on the sphere by applying the frequency-domain atmospheric absorption correction of Bass et al. (Ref. 20) to the spectra for a reference distance of 1 m. The resulting spectra can also be A-weighted and summed, since both the atmospheric absorption and the A-weighting filters are linear. The difference between the A-weighted noise level and the A-weighted noise level including 1 m of atmospheric attenuation is the excess atmospheric attenuation factor. The excess atmospheric attenuation factor represents the attenuation of the A-weighted level due to atmospheric absorption for each meter of propagation, and is calculated separately for the spectrum associated with each emission angle and flight condition of the helicopter in the database. This approach requires only a single calculation for straight ray propagation from the source spheres to an observer on the ground, instead of requiring a separate calculation for each harmonic contained in the original frequency spectrum.

Due to the computational efficiency of the noise model, it is now practical to adjust the flight trajectory using a numerical optimizer in order to identify low noise optimal maneuvers. A flowchart of the FRAME-QS method used in this paper is shown in Figure 2, with the components of the optimization

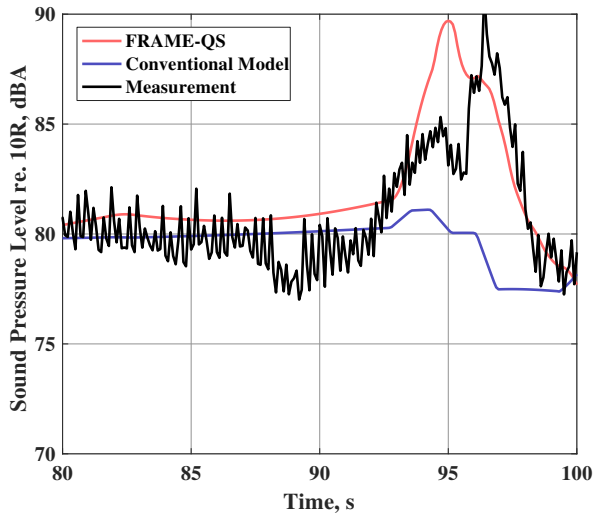

(a) Fast pitch up.

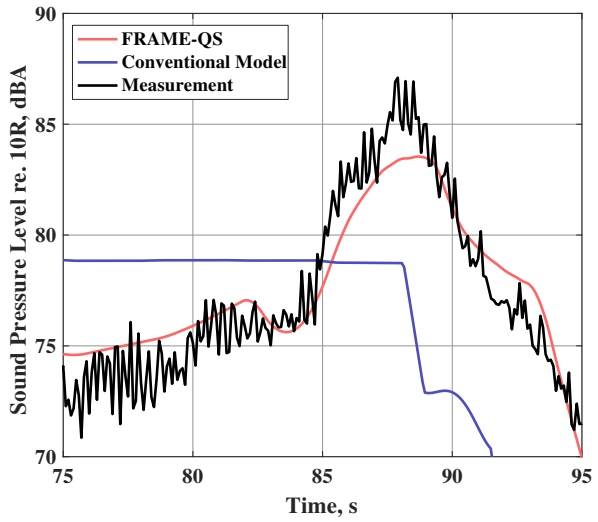

(b) Advancing side roll maneuver.

Fig. 1. Comparison of FRAME-QS model to conventional modeling and measured data (from Ref. 17).

approach highlighted. Following the so-called "direct method" in optimal control theory (Ref. 21), each trajectory is defined by a set of control points that set the position and time of the boundaries of the quintic spline segments that form the continuous helicopter flight trajectory. A hybrid optimization approach is used to adjust these control points because the low noise trajectory optimization problem is not convex, i.e., there exist many local minimum noise solutions, such that a conventional gradient based optimizer is unlikely to achieve significant progress in reducing noise on the ground.

The hybrid optimization begins with a probabilistic global optimization method called Adaptive Simulated Annealing (ASA) (Ref. 22). ASA is a metaheuristic that works by perturbing the current solution in a random direction—the optimizer will compare the new and old solutions and is most likely to select the position that is "better" (i.e., has a lower noise metric). However, there is some random chance that the optimizer will instead select the "worse" solution, in hope that it will allow the optimizer to escape a local minimum. The probability of the optimizer selecting the "worse" solution is based

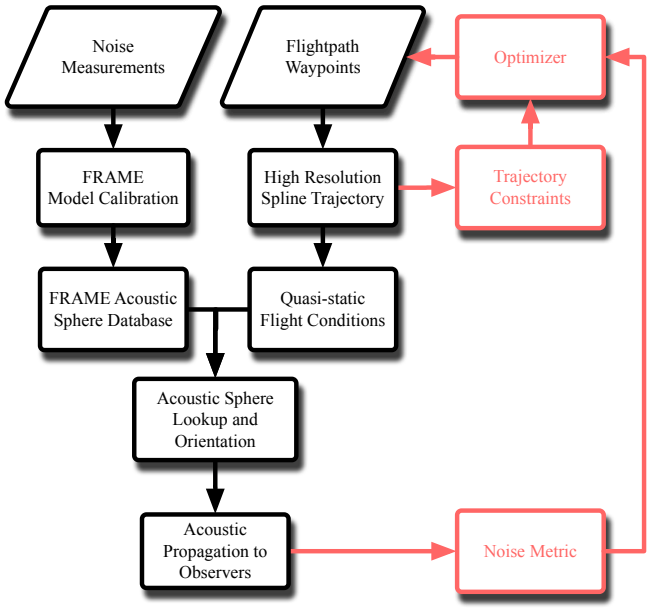

Fig. 2. Flow chart of FRAME-QS trajectory optimization.

on a parameter called the "temperature." The "temperature" starts out high, which causes the optimizer to take a higher proportion of exploratory moves toward "worse" solutions. As the solver iterates, the "temperature" is decreased, and ASA refines the solution. Once that solution converges, the "temperature" is restarted to a high value, and the process begins again. Because this type of global optimization is relatively inefficient on smooth problems, each time ASA converges to a local solution, it is further refined using a conventional gradient based optimization approach, Sequential Quadratic Programming (SQP) (Ref. 23).

The objective function for the optimization can be defined using any number of noise metrics; however, because the noise model only predicts A-weighted SPL on the ground throughout the trajectory, the metric must be derived from this data. For example, commonly used community noise metrics such as the maximum A-weighted noise level, equivalent noise level, or Sound Exposure Level (SEL) may be combined over all or part of the analysis area to form a single noise metric for the entire trajectory. Additionally, constraints must be imposed on the trajectory to keep solutions within the bounds of practicality. These constraints include limitations on the minimum altitude, the maximum speed, the pitch angle of the helicopter (which implicitly limits longitudinal acceleration and flight path angle), and the load factor of the main rotor. These constraints can be explicitly handled by the SQP portion of the optimizer; however, they are implemented in the ASA optimization through the use of extended interior penalty functions (Ref. 24).

RESULTS

Evaluation of Flight Procedure Variations

The model described in the previous section is applied in this section to evaluate community noise exposure for several representative flight procedures for the AS350 SD1 helicopter,

including longitudinal accelerations, climbs, and turns, and the acoustic effects of variations on these maneuvers. The FRAME acoustic sphere database for the AS350 SD1 was previously constructed and validated (Ref. 25) using data collected by NASA and the Army for the AS350 SD1 at Salton Sea in 2015 (Ref. 26). The noise model predicts the A-weighted SPL at 0.25 second intervals over the duration of the maneuver for 2500 observers arranged in a 2 km square grid set on a hard ground plane. The community noise impact of the entire maneuver can be quantified using the Sound Exposure Level (SEL) metric, which is calculated from the predicted A-weighted SPL over the interval where levels are within 10 dB of the peak level and are normalized to a duration of one second. Due to the computational efficiency of the noise model, complete ground noise contours can be evaluated more than 450 times faster than real time using a single 2.5 GHz Intel Core i7 CPU core.

Longitudinal Acceleration / Deceleration ("Quick Stop")

The first flight procedures evaluated are representative of constant altitude longitudinal acceleration and deceleration, or "quick stop," maneuvers from straight level flight conditions at an altitude of 250 m (820 ft) above the ground plane. The SEL contours for these maneuvers are shown in Figure 3, along with the ground track of the helicopter during the maneuver. In all four cases, the helicopter begins the trajectory flying at 40 m/s (78 kts) in the X direction. After ten seconds of steady flight, in three of the cases the helicopter begins a longitudinal acceleration or deceleration at X = -1000 m (-3280 ft). A constant acceleration or deceleration is established and maintained until X = 0 m, at which point the helicopter returns to steady constant speed flight for another ten seconds. Figure 3a shows the SEL contours for the baseline case where the helicopter maintains constant speed throughout the trajectory, resulting in relatively constant sideline noise levels along the trajectory X = -1000 m to 0 m (-3280 ft to 0 ft). Figure 3b shows the SEL contours for a moderate acceleration of 0.05g. Compared to the steady flight baseline, Figure 3a, the noise contours slightly widen near the end of the trajectory as the helicopter picks up speed and the noise radiated forward increases. Conversely, the mild deceleration maneuver results in an increase in SEL for observers near the beginning of the maneuver, shown in Figure 3c, while noise levels near the end of the maneuver are decreased due to the reduction in speed. However, a moderate deceleration "quick stop" of 0.1g shows (Figure 3d) a large increase in noise levels relative to the constant speed baseline throughout entire observer area.

These trends can be explained by examining the A-weighted SPL contours associated with specific times of emission during the maneuvers. Figure 4 compares the A-weighted SPL noise contours of the helicopter just prior to the acceleration maneuver (Figure 4a) with those at nearly the same speed just after the various accelerations are established (Figures 4b to 4d). The moderate forward acceleration of the helicopter—shown in Figure 4b—initially causes little change in radiated noise levels relative to constant speed flight (Figure 4a). However,

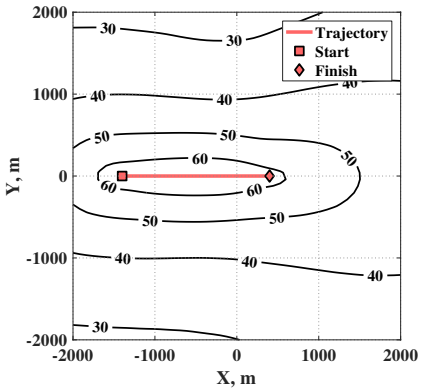

(a) Constant speed.

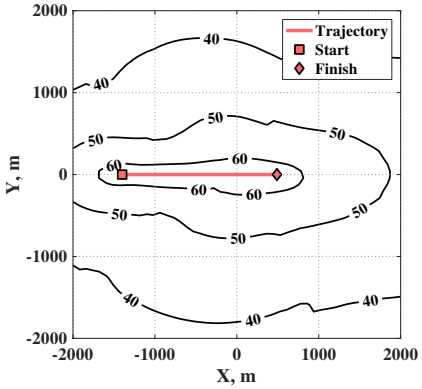

(b) 0.05g acceleration.

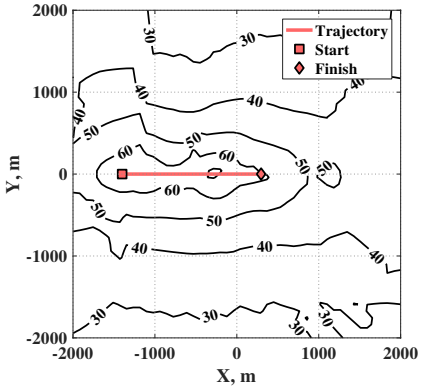

(c) 0.05g deceleration.

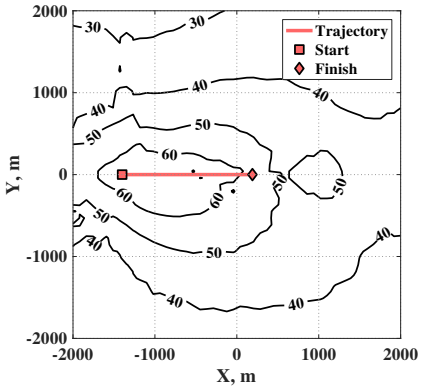

(d) 0.1g deceleration.

Fig. 3. Sound Exposure Level contours (dBA) for longitudinal acceleration or deceleration from 40 m/s (78 kts).

a mild deceleration causes a significant increase in radiated noise levels, shown in Figure 4c. This is because the helicopter rotor must tilt rearwards to decelerate the helicopter, increasing the rotor angle of attack and, therefore, decreasing the "miss-distance" between the rotor tip-path-plane and the rotor wake, leading to the onset of BVI noise. Greater deceleration, Figure 4d, causes an even larger increase in A-weighted noise levels as the effective flight path angle of the helicopter approaches the maximum BVI flight path angle of -8°. For observer locations within 1000 m (3280 ft) of the flight track, the peak A-weighted noise levels for the 0.1g deceleration are nearly 20 dBA higher than for the constant speed flight case.

Pitch Up into Climb

The next type of maneuver which is evaluated is a pitch up into a climb from a steady level flight condition. Two climbs are evaluated: a shallow climb, at a 6° flight path angle, and a steep climb at a 12° flight path angle. Figure 5 plots the vertical component of the trajectories of the two climb maneuvers. Once again, the helicopter begins the simulated maneuver at 40 m/s (78 kts) flight in the X-direction at 250 m (820 ft) altitude above the ground plane. The helicopter maintains this condition for 10 seconds, and then begins to climb at X = -1000 m (-3280 ft). The helicopter establishes a constant flight path angle climb until reducing the flight path angle to establish level flight at X = 0 m. The level flight condition is then maintained for another 10 seconds.

Figure 6 compares the SEL contours for a shallow 6° flight path angle climb (Figure 6a) with that of a steep 12° flight path angle climb (Figure 6b). The SEL contours are relatively insensitive to changes in the climb angle; there is some reduction in SEL on the sideline of the center (constant climb angle) section of the steep climb maneuver, but SEL near either end of the trajectory are comparable.

Instantaneous A-weighted SPL for several times of emission during the steep climb maneuver are shown in Figure 7. Figure 7a shows the SPL associated with the steady flight condition of the helicopter just prior to X = -1000 m (-3280 ft). The noise radiated forward of the helicopter increases during the pull up to the steep climb, shown in Figure 7b, because the pull up increases the both the tip-path-plane angle of attack of the rotor and the rotor load factor, leading to increased loading noise generation. Once the climb is established, shown in Figure 7c, noise levels observed at points on the ground that are far from the helicopter are comparable to those predicted for the steady flight segment (Figure 7a) at the beginning of the maneuver; however, there is a 3 dBA decrease in noise levels observed directly underneath the helicopter caused by increased propagation losses because the altitude has increased from 250 m to 350 m (820 ft to 1150 ft). The are no significant changes in noise caused by the pitch down of the helicopter to the steady flight segment at the end of the maneuver, as shown in 7d, other than further reductions in levels directly under the helicopter due to the increase in altitude.

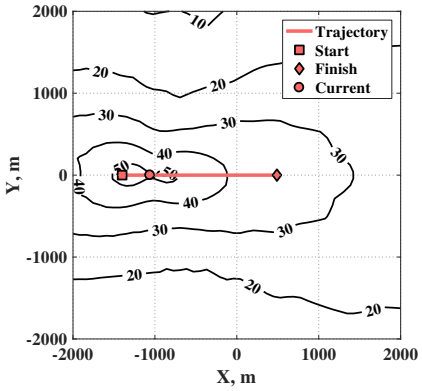

(a) Prior to acceleration maneuver.

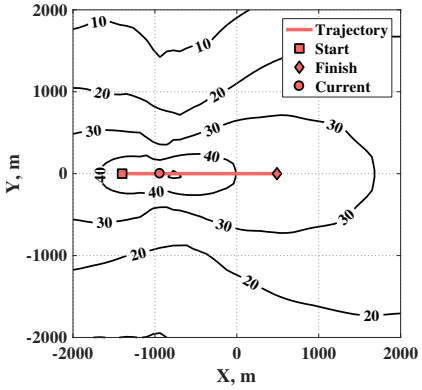

(b) Start of 0.05g acceleration maneuver.

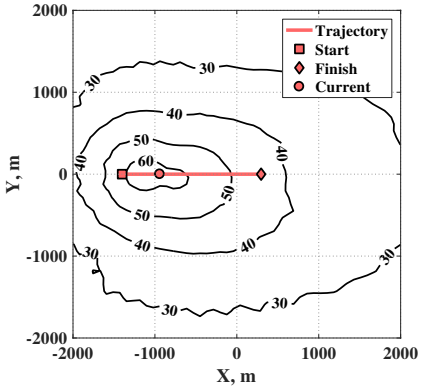

(c) Start of 0.05g deceleration.

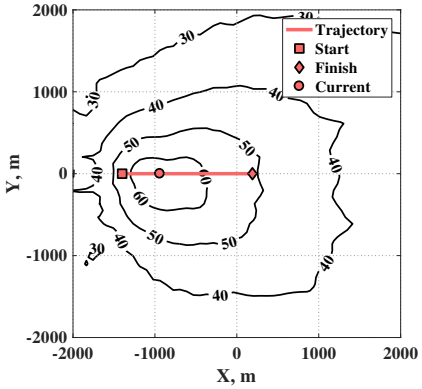

(d) Start of 0.1g deceleration.

Fig. 4. A-weighted ground noise contours (dBA) at emission times before and after initiation of longitudinal acceleration or deceleration.

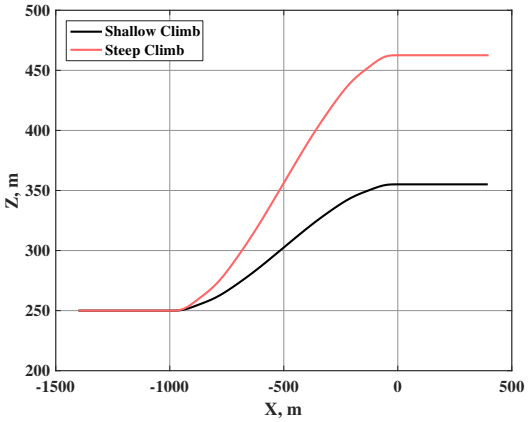

Fig. 5. Comparison of climb trajectories.

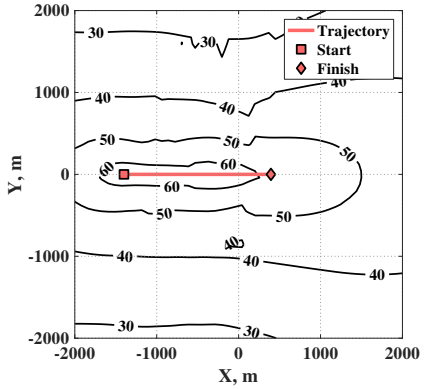

(a) Shallow climb.

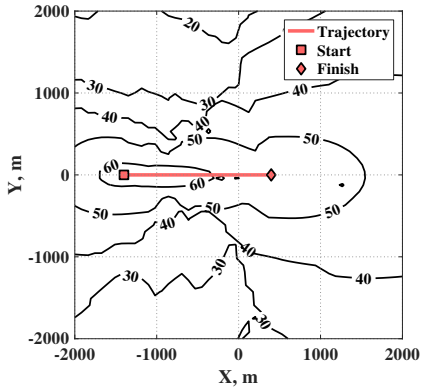

(b) Steep climb.

Fig. 6. Sound Exposure Level contours (dBA) for climbs from 40 m/s (78 kts) level flight.

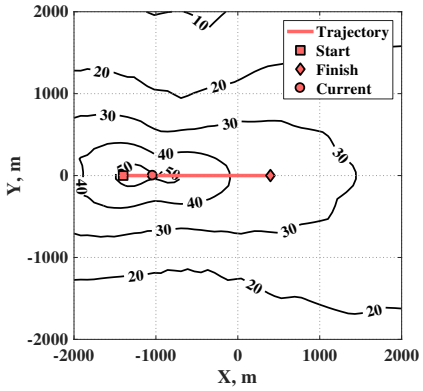

(a) Before start of climb.

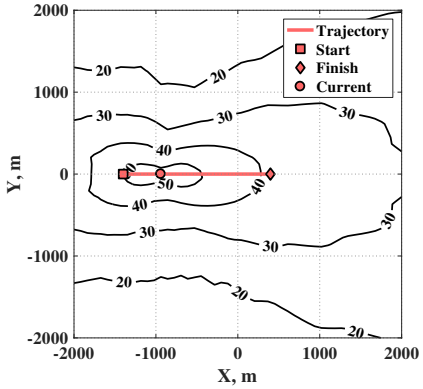

(b) During pull up to steep climb.

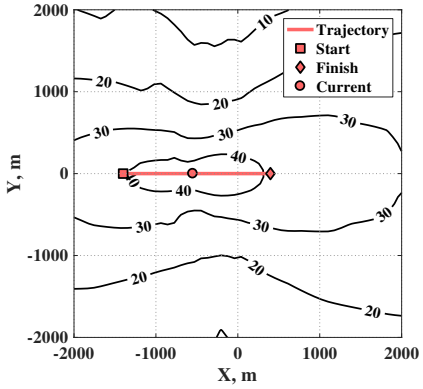

(c) During steep climb.

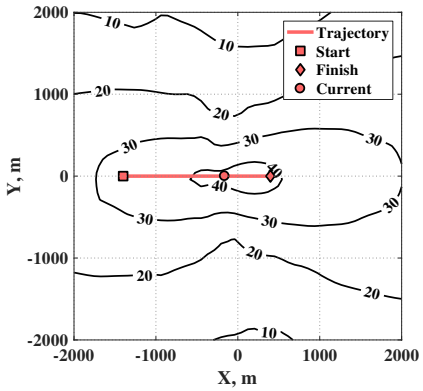

(d) After exit from steep climb.

Fig. 7. A-weighted ground noise contours (dBA) at several times of emission during steep climb maneuver.

Level Turn

The next type of flight procedure considered is a level turn. The level turn once again starts with 10 seconds of level flight at 40 m/s (78 kts) in the X direction. The level turns are conducted at an altitude of 250 m (820 ft) above the ground plane. The turn starts at X = -1000 m (-3280 ft), and continues through 90° of heading change, ending at X = 0 m. Figure 8 plots the SEL contours for six variations on the level turn. The upper row of figures, Figures 8a to 8c, show the trajectories and SEL for turns toward the advancing side (left) of the helicopter. Likewise, Figures 8d to 8f show trajectories and SEL for turns toward the retreating side (right) of the helicopter. For each turn direction, turn maneuvers are conducted with three different constant accelerations: 0.1g deceleration (Figures 8a and 8d), constant speed (Figures 8b and 8e), and 0.1g acceleration (Figures 8c and 8f).

The decelerating turn toward the advancing side results in large increases in SEL of more than 10 dBA for observers outside of the turn, as compared to the constant speed case (Figure 8b). This increase is especially apparent at sideline locations near the early portion of the trajectory. Noise levels inside of the turn do not increase by as much in response to the deceleration of the helicopter. In the case of the accelerating turn toward the advancing side, Figure 8c, there is a 4 dBA decrease in SEL underneath X = -1000 m (-3280 ft), where the helicopter rolls into the turn, relative to the constant speed case. However, there are significant increases in SEL to both sides of the later portion of the flight track, by as much as 20 dBA for far away observers on the inside portion of the turn. The constant speed turn toward the retreating side, Figure 8e, results in similar SEL to the constant speed turn toward the advancing side, Figure 8b. Similarly, the SEL contours for the accelerating turn toward the retreating side, Figure 8f, show the same trends as for the accelerating turn toward the advancing side, Figure 8c. However, the increase in noise levels caused by deceleration is significantly reduced for the turn toward the retreating side, Figure 8d, as compared to the turn toward the advancing side, Figure 8a. In all turning flight cases, sideline noise levels are higher for turning flight than for steady straight line flight (shown previously in Figure 3a)–for instance, the SEL average 4 dBA higher to the sideline of the constant speed turn (Figure 8b) than for steady straight line flight at the same speed.

To better understand the noise radiation of the turning helicopter over time, Figure 9 plots the A-weighted SPL contours associated with several times of emission for both the constant speed (Figures 9a to 9c) and decelerating (Figures 9d to 9f) turns. Figure 9a shows the SPL observed on the ground at the moment when the helicopter rolls into the advancing side turn. Noise levels are as many as 10 dBA higher toward the outside of the roll-in than toward the inside at the same sideline distance. Noise levels are higher for the roll-in than for the "steady" midpoint of the turn, shown in Figure 9b, where a constant bank angle of about 20° is reached. Noise levels are slightly lower during this "steady" portion of the turn, on average by about 3 dBA throughout the observer grid. During the roll-out of the turn, SPL levels decrease even further, by another 2 dBA on average over the turn midpoint.

Figure 9d shows the time of emission SPL contours for the roll-in to the decelerating turn. A large increase in noise levels is observed toward the outside of the roll-in due to the onset of strong BVI caused by the combination of deceleration and roll toward the advancing side of the rotor that reduces rotor-wake "miss-distance"; these noise levels are much greater than for the constant speed roll-in shown in Figure 9a. However, the SPL contours associated with the midpoint time of emission are not much different for the constant speed (Figure 9b) and decelerating (Figure 9e) cases. During the roll-out of the turn, the decelerating case results in higher levels of noise radiation behind the helicopter (Figure 9f) but relatively small changes ahead of the helicopter relative to the constant speed case shown in Figure 9c. This is largely because the reduced speed of the decelerating helicopter near the endpoint of the trajectory causes an increase in the retreating blade tip Mach number and a corresponding increase in noise levels radiated rearwards.

Climbing/Descending Turn

The last type of maneuver evaluated in this section is the combination turn and climb or descent. Figure 10 plots the SEL contours for 40 m/s (78 kts) turns at several different flight path angles ranging from a shallow climb (+3°) to a moderate descent(-6°). The steady constant speed turn shown originally in Figure 8b is repeated in Figure 10b to facilitate the comparison. Once again, the helicopter maintains a steady flight condition for 10 seconds at either end of the trajectory; however, in this case the steady segment is climbing or descending at the same flight path angle as the rest of the turn. The starting and exit altitudes are varied such that the average height of the climbing or descending turn is held at 250 m (820 ft).

The climbing turn, shown in Figure 10a, yields similar SEL as the level turn for most of the maneuver, but SEL decrease directly underneath the helicopter near the end of the climb trajectory due to the increase in altitude. However, the noise radiation for the descending turn is on average 10 dBA higher across the observer grid due to the increase in BVI, especially during the roll-in and roll-out of the turn. Further increases in SEL are observed for the -6° flight path angle turn, shown in Figure 10d. SEL are, on average, another 5 dBA higher for the moderate descending turn than the gently descending turn.

Noise Abatement Flight Procedure Guidance

The results of application of the FRAME-QS model to maneuvering flight procedures can be used to provide some general advice for helicopter pilots seeking to reduce community exposure to objectionable noise:

- Decelerations, even of moderate magnitudes of 0.1 g or less, can cause significant increases in A-weighted noise levels due to the onset of BVI. Pilots should be careful to avoid the natural tendency to decelerate into other maneuvers, such as turns or pull ups, where BVI noise is more likely to occur.

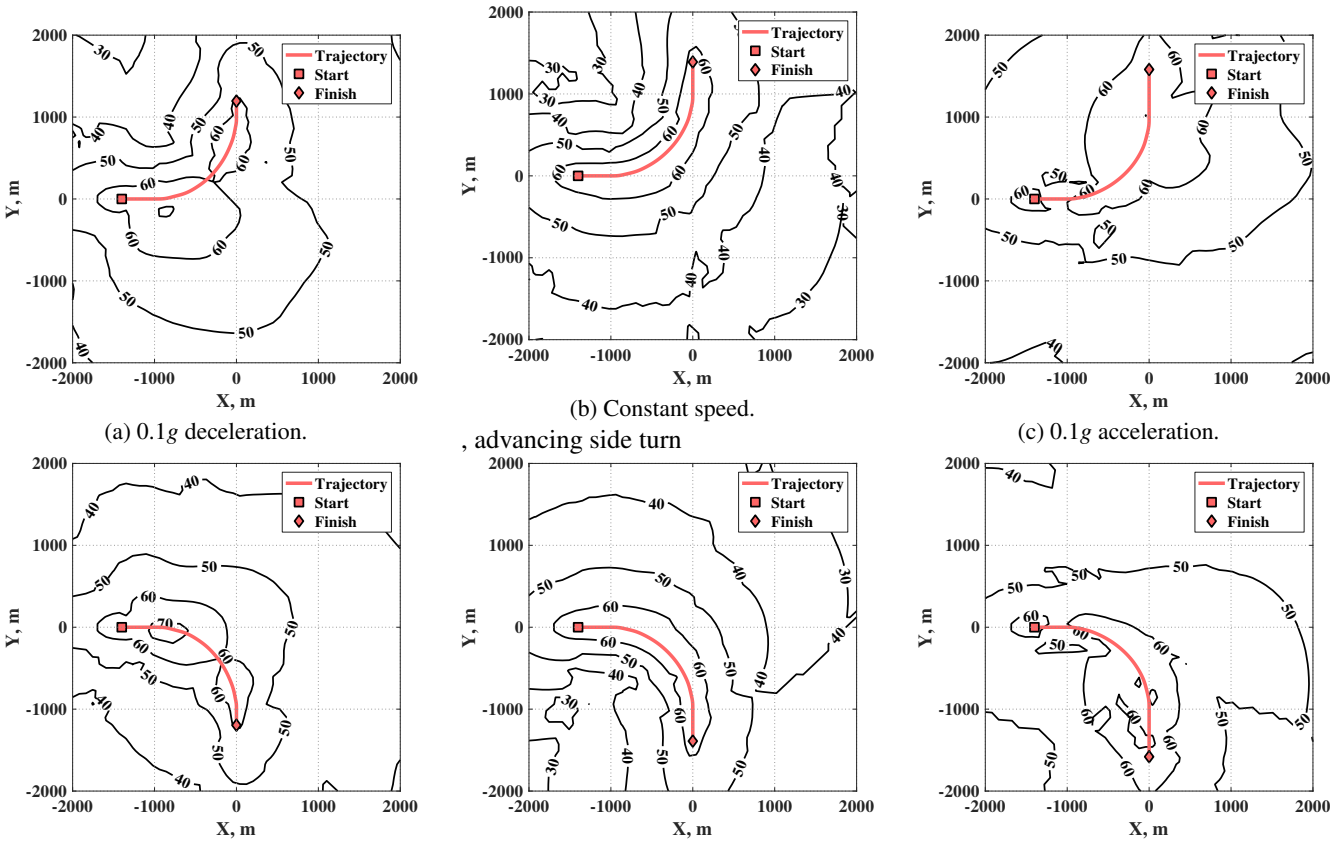

(a) 0.1g deceleration. (b) Constant speed. (c) 0.1g acceleration.

, advancing side turn

(d) 0.1g deceleration. (e) Constant speed. (f) 0.1g acceleration.

Fig. 8. Sound Exposure Level contours (dBA) for level turns from 40 m/s (78 kts) straight flight. Figures 8a to 8c are toward the advancing side of the rotor (left) and Figures 8d to 8f are toward the retreating side (right).

- Acceleration does not lead to substantial reductions in noise during level flight, where BVI does not typically occur, but may still be useful to increase the "miss-distance" margin from BVI-prone flight conditions during maneuvers, such as the roll-in to a turn. However, acceleration should not be sustained throughout the duration of turns or other maneuvers as the increased flight speed will result in higher noise radiated ahead of the helicopter.

- Noise levels on the outside of a turn are generally higher than toward the inside of a turn, due to the banking of the helicopter directing main rotor loading and tail rotor thickness noise toward the outside of the turn. Noise levels during turning flight are higher than for similar straight line flight conditions. Turns should be avoided near noise sensitive areas; when turns must be made near noise sensitive areas, the acoustic impact is minimized by keeping the noise sensitive region toward the inside of the turn.

- BVI noise caused by the roll-in or out of a turn is increased for turns toward the advancing side of the rotor. Advancing side turns should not be combined with deceleration or descents when possible. However, advancing side turns are not much louder than retreating side turns during accelerating or climbing turns, where BVI is more easily avoided.

- Rotor harmonic noise levels are relatively insensitive to the rate of climb, although the initial rate of increase of the flight path angle should be limited to avoid unnecessary deceleration. Steeper climbs allow the helicopter to increase altitude more quickly, reducing noise levels directly beneath the flight track. However, attenuation of noise levels has diminishing returns with increasing altitude due to the logarithmic nature of spherical spreading losses. Moreover, increased altitude provides little noise benefit to observers who are far from the flight path.

Low Noise Optimal Flight Procedures

The degree to which the noise generated by helicopter maneuvers can be reduced through changes in flight procedures is assessed in this section of the paper. Due to computational efficiency of the FRAME-QS model and its applicability to maneuvering flight, numerical optimization can be applied to the model on a practical time scale to devise low noise flight procedures using the methods described in the Approach section. Three different flight procedures will be examined; a level turn, a straight line approach to a hover taxi, and a turning approach to a hover taxi. In all three cases, the trajectory is described using splines with ten defined control points. Because each control point is defined by the time, and X, Y, and Z positions, there are forty design variables in total. The initial trajectory

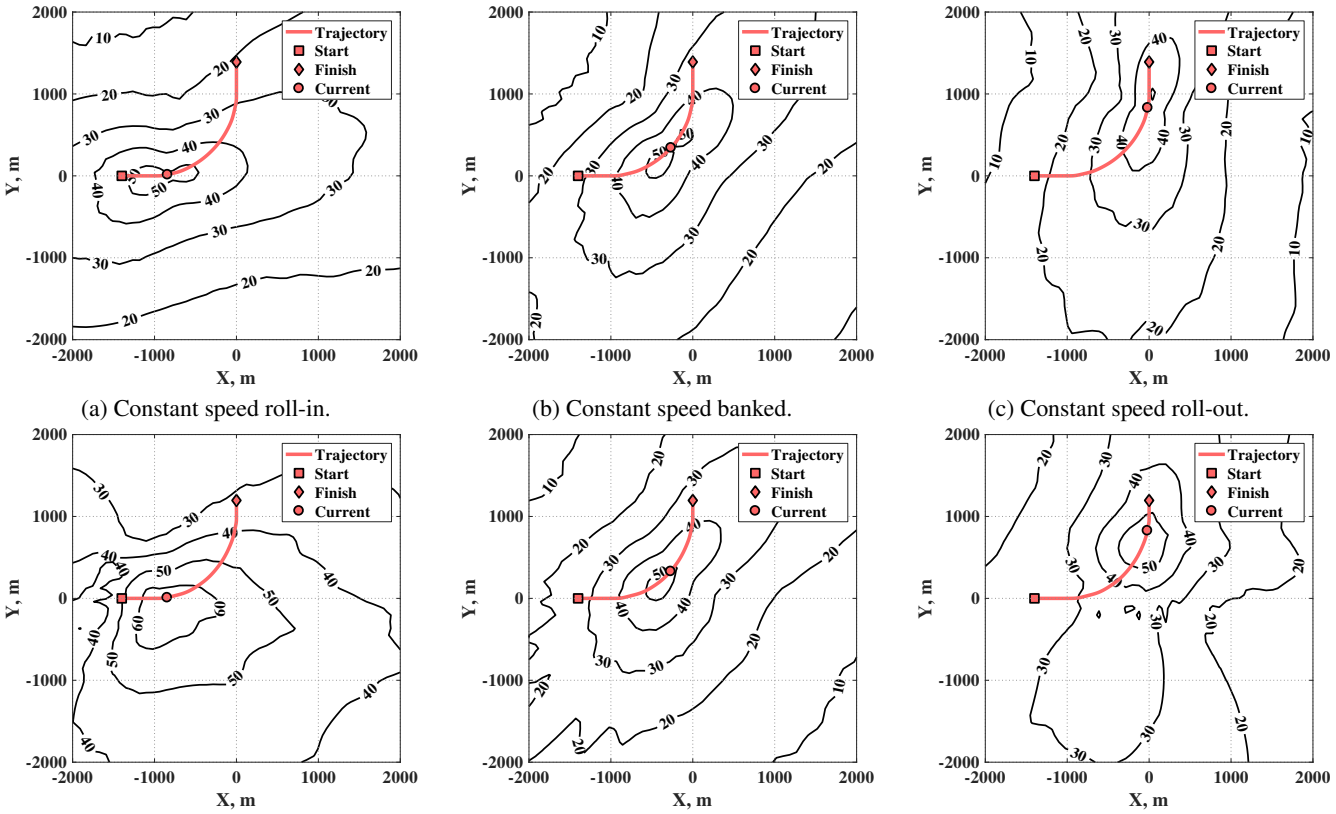

(a) Constant speed roll-in. (b) Constant speed banked. (c) Constant speed roll-out.

(d) Decelerating roll-in. (e) Decelerating banked. (f) Decelerating roll-out.

Fig. 9. A-weighted ground noise contours (dBA) at several times of emission during constant speed and decelerating advancing side turn maneuvers from 40 m/s (78 kts) straight and level flight.

is defined analytically as the cubic polynomial in time that connects the defined starting position and velocity to the final position and velocity. The optimizer seeks to reduce the mean SEL across the observer grid, while still meeting the following trajectory constraints for safety and comfort: a minimum altitude of 5 m (16 ft), a maximum speed of 65 m/s (126 kts), a minimum load factor of 0.8, a maximum load factor of 1.4, a minimum pitch angle of -20°, and a maximum pitch angle of 10°. Each case required between 10,000 and 20,000 iterations to achieve convergence, using several hours of CPU time for each run.

Level Turn

The first case examined is a level quarter-turn toward the advancing side starting and ending at an airspeed of 50 m/s (97 kts) and altitude of 50 m (194 ft) above the ground plane. Figure 11 compares the SEL predicted for the initial trajectory (Figure 11a) with the optimized trajectory (Figure 11b). The optimized maneuver results in a reduction in the average SEL across the observer grid of 5 dBA over that of the initial trajectory.

Figure 12 compares the variations in the speed and bank angle of the initial flight procedure with the optimized one over the duration of the maneuver. Instead of maintaining constant speed, the optimized maneuver decelerates at the fastest rate possible prior to the onset of BVI (Figure 12a) in order to reduce the speed of the helicopter throughout the turn. After the deceleration is largely complete, the optimized trajectory rolls into the turn (Figure 12b) at low speed. Due to the nature of the spline basis functions, the optimal solution exhibits mild oscillatory behavior; however, the resulting trajectories are still well within the previously defined safety and comfort constraints. Because the speed of the helicopter is lower in the optimized maneuver than for the initial case, the roll rate and maximum bank angle reached during the optimized maneuver is reduced by half. Midway through the turn, the helicopter begins a gradual acceleration which is maintained throughout the roll-out of the turn, in order to reduce BVI noise through the maneuver. Because of the lower average speed, the optimized maneuver occurs over a 20% longer duration. The community impact of the increased duration of noise exposure is reflected in the SEL metric plotted in Figure 11.

Straight Approach to Hover Taxi

The noise optimization is next applied to a straight approach to a hover taxi. The helicopter starts at an altitude of 150 m (492 ft), flying at a velocity of 50 m/s (97 kts) along a -6° flight path angle glide slope toward the X direction. The trajectory ends 2000 m (6560 ft) further in the X direction in level flight at an altitude of 10 m (33 ft) and a speed of 7.5 m/s (15 kts). Figure 13 shows the SEL contours for the initial approach trajectory versus the optimized approach trajectory. The op-

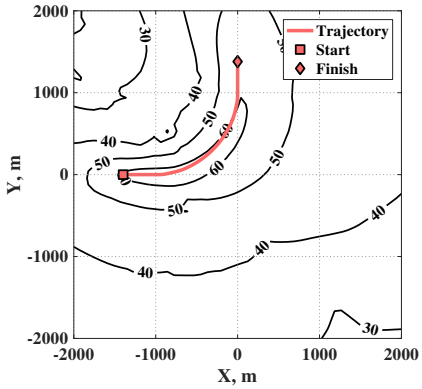

(a) Climbing, +3° flight path angle.

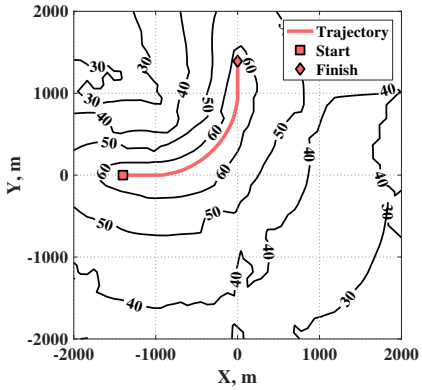

(b) Level, 0° flight path angle.

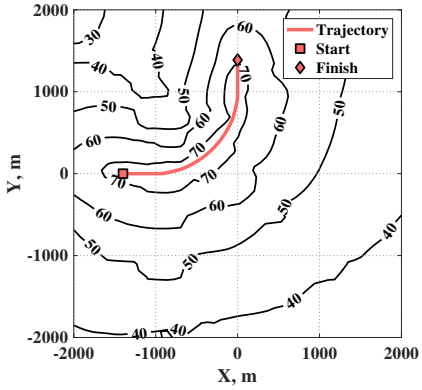

(c) Descending, -3° flight path angle.

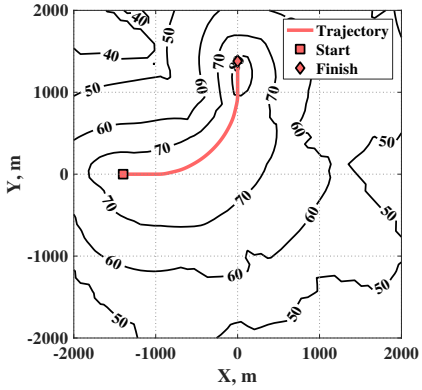

(d) Descending, -6° flight path angle.

Fig. 10. Sound Exposure Level contours (dBA) for climbing, level, and descending turns at 40 m/s (78 kts) constant speed.

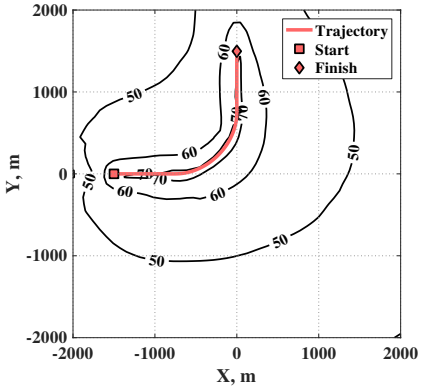

(a) Initial.

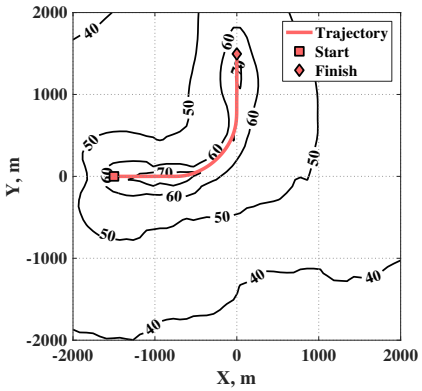

(b) Optimized.

Fig. 11. Sound Exposure Level contours (dBA) for initial and optimized level turns.

timized approach trajectory reduces the mean SEL over the observer area by 7 dBA from the initial trajectory. Noise reductions are seen throughout the observer grid, but are weighted toward the later portion of the trajectory.

Figure 14 compares the variation in velocity and flight path angle between the initial and optimized approach procedures. The initial procedure maintains a constant rate of deceleration throughout most of the trajectory, as shown in Figure 14a. In contrast, the optimized approach decelerates more aggressively in the initial portion of the maneuver, when the helicopter is high above the ground plane, allowing a reduced rate of deceleration closer to the approach area and a lower average speed throughout. Consequently, the optimized approach is able to descend more steeply near the end of the flight trajectory—shown in terms of flight path angle in Figure 14b and in height in Figure 14c—before encountering high levels of BVI noise.

Turning Approach to Hover Taxi

The final optimized flight procedure considered is a combined approach and quarter turn toward the advancing side of the helicopter. As for the straight approach, the maneuver starts at a 150 m (492 ft) altitude at a speed of 50 m/s (97 kts) along a -6° flight path angle, and terminates in level flight at an altitude of 10 m (33 ft) and a speed of 7.5 m/s (15 kts). The SEL contours for the initial and optimized maneuvers are shown in Figure 15. The optimized maneuver results in a mean SEL

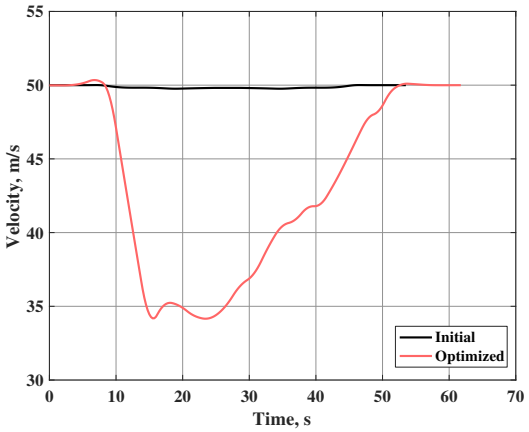

(a) Velocity variation.

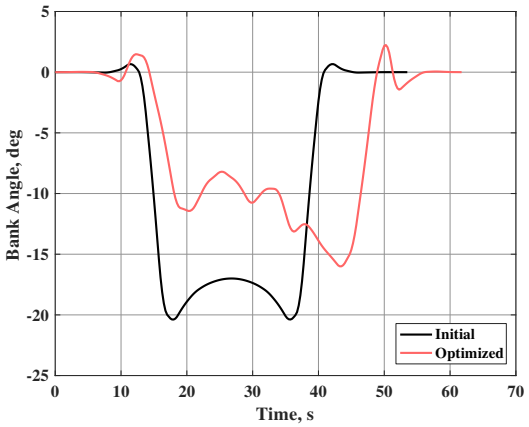

(b) Bank angle variation.

Fig. 12. Variation in flight parameters between initial and optimized turn maneuvers.

reduction of 10 dBA over the observer grid, with the largest reductions seen near the end of the trajectory.

Figure 16 compares the variation in velocity, bank angle, and altitude between the initial and optimized turning approach maneuvers. Much like in the previous cases, this reduction is achieved through early deceleration, shown in Figure 16a, prior to the roll-in to the turn. Due to the reduced speed, the roll rate and maximum bank angle (Figure 16b) of the optimized turn are reduced compared to the initial solution. The deceleration is reduced midway through the turn as a gradual roll-out of the turn is accomplished at a reduced rate of descent (Figure 16c) relative to the initial trajectory.

The optimized maneuvers developed in this section demonstrate that large reductions in SEL can be achieved over a wide area by tailoring maneuvering flight procedures for low noise operations. The optimized procedures work primarily through conducting necessary deceleration at the highest point in the trajectory, separating deceleration from other maneuvers, maintaining low speeds during turns and when near the ground, and through limited acceleration during the transition from turning flight to straight and level flight. These noise optimal maneuvers are likely to be situation specific and require too high a pilot workload to achieve maximum effectiveness in noise reduction for conventional helicopters. However, optimal maneuvers like these may be enabled through future

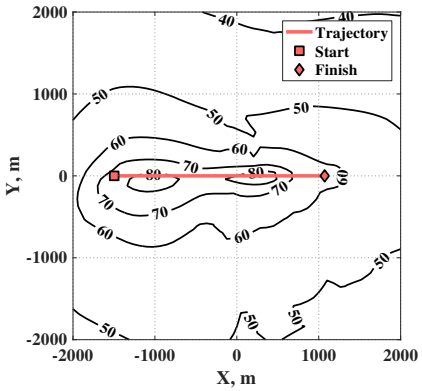

(a) Initial.

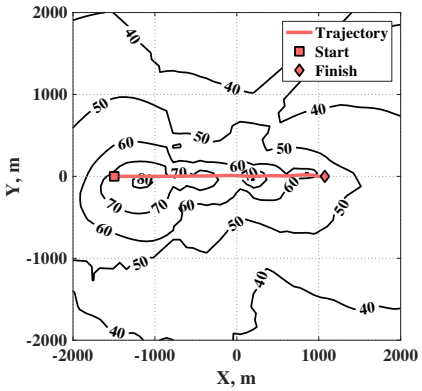

(b) Optimized.

Fig. 13. Sound Exposure Level contours (dBA) for initial and optimized straight approaches.

developments of pilot guidance displays (Ref. 27) or through autonomous or semi-autonomous helicopter operations.

CONCLUSIONS

The previously validated FRAME-QS model, in conjunction with a computationally efficient propagation model, was applied to develop guidelines for helicopter maneuvering flight operations with reduced community noise impact. Transient maneuvers can result in significant changes in time-averaged SEL—a primary noise metric used to assess community annoyance in response to aircraft noise—in addition to their effect on instantaneous SPL. Relatively small changes to these maneuvering flight procedures can result in large changes in SEL, as much as 20 dBA for certain observers. Helicopter noise assessment tools must capture the effects of transient maneuvers in order to adequately resolve community noise impacts.

Pilots can effectively limit the adverse effects of helicopter noise radiation by changing their flight procedures. Critically, pilots should avoid entering or exiting turning flight while decelerating or descending. When operating near noise sensitive areas, turns should be conducted such that noise sensitive areas are located on the inside of the turn, and preferably toward the retreating side of the helicopter.

Further reductions in SEL can be achieved through the identification of low noise optimal maneuvers. However, the benefits of such maneuvers cannot be practically realized by developing noise optimal maneuvers offline to be flown later by unaided

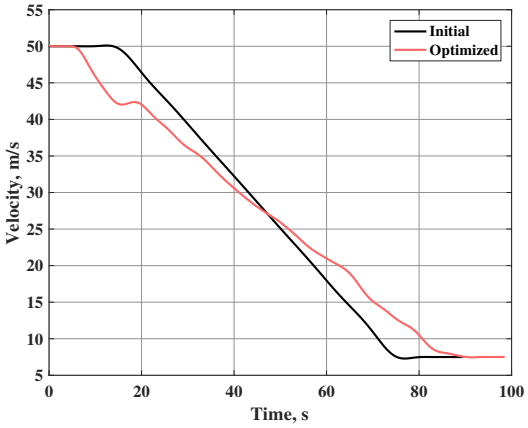

(a) Velocity variation.

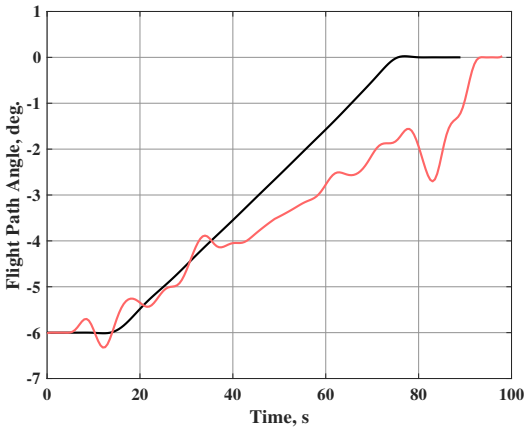

(b) Flight path angle variation.

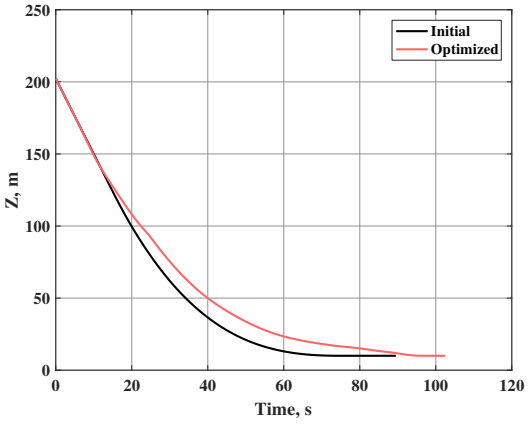

(c) Altitude variation.

Fig. 14. Variation in flight parameters between initial and optimized approach maneuvers.

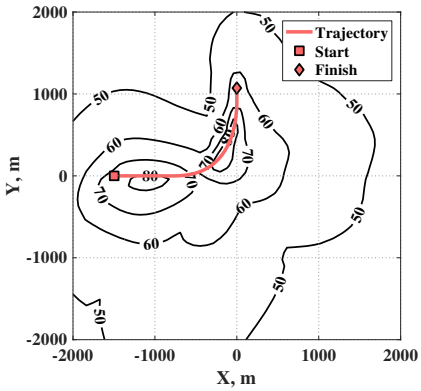

(a) Initial.

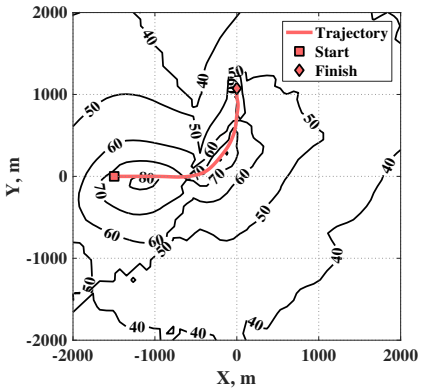

(b) Optimized.

Fig. 15. Sound Exposure Level contours (dBA) for initial and optimized turn and approach maneuvers.

pilots. Instead, future helicopters with greater autonomy must be capable of developing effective low noise procedures during flight that also safely accomplish the objectives of the operator. Despite great improvements in the computational efficiency of accurate semiempirical helicopter noise models, such as FRAME-QS, the time required to perform direct trajectory optimization including acoustic considerations is still much too great to provide near-time noise abatement guidance. More effective trajectory optimization algorithms, and perhaps greater onboard computational power, are required in order to consistently achieve the maximum benefit of helicopter noise abatement procedures.

ACKNOWLEDGMENTS

The author would like to thank Mr. Michael E. Watts, NASA Langley Research Center, and Drs. Ben W. Sim and James H. Stephenson, US Army Aviation Development Directorate, for providing helpful discussion and insights during the prepatation of this paper.

Author Contact

Eric Greenwood, eric.greenwood@nasa.gov

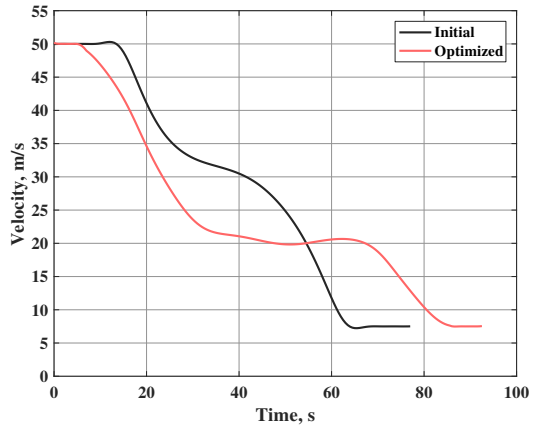

(a) Velocity variation.

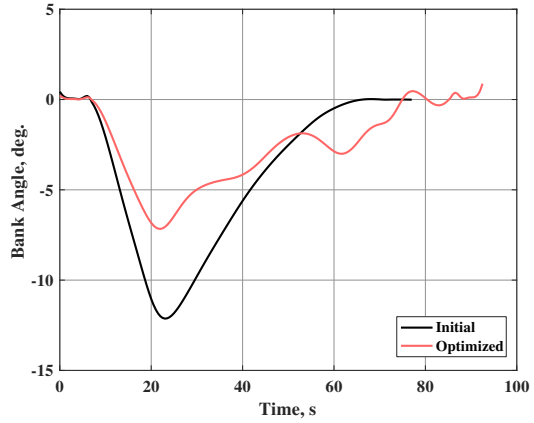

(b) Bank angle variation.

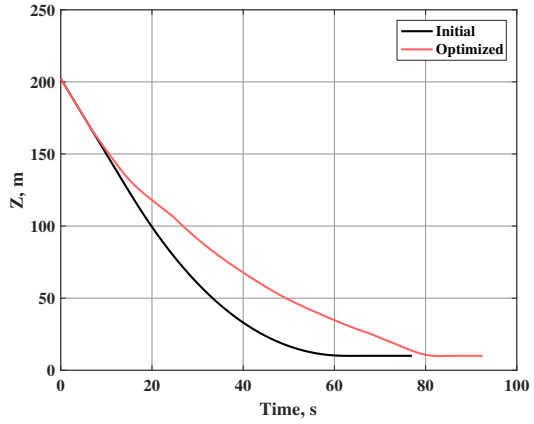

(c) Altitude variation.

Fig. 16. Variation in flight parameters between initial and optimized approach maneuvers.

REFERENCES

[1]"LA Helicopter Noise Initiative," http://heli-noise-la.com, Accessed: 2017-03-05.

[2]"Westchester County Airport Noise Abatement," http://airport.westchestergov.com/environmental-management-system/noise-abatement, Accessed: 2017-03-05.

[3]"NYCEDC And Helicopter Tourism & Jobs Council Announce New Measures to Reduce Helicopter Noise And Impacts Across New York City," https://www.nycedc.com/press-release/nycedc-and-helicopter-tourism-jobs-council-announce-new-measures-reduce-helicopter, Accessed: 2017-03-05, February 2016.

[4]Visser, H. G., Pavel, M. D., and Tang, S. F., "Optimization of Rotorcraft Simultaneous Noninterfering Noise Abatement Approach Procedures," *Journal of Aircraft*, Vol. 46, (6), August 2009, pp. 2156–2161.

[5]Padula, S. L., Burley, C. L., Boyd Jr, D. D., and Marcolini, M. A., "Design of Quiet Rotorcraft Approach Trajectories," Technical Report TM-2009-215771, NASA, 2009.

[6]Hindson, W. S. and Chen, R. T. N., "Operational Tests of Noise Abatement Approaches for Rotorcraft Using Differential GPS for Guidance," *Journal of the American Helicopter Society*, Vol. 43, (4), 1998, pp. 352–359.

[7]Jacobs, E. W., Prillwitz, R. D., Chen, R. T. N., Hindson, W. S., and Santa Maria, O. L., "The Development and Flight Test Demonstration of Noise Abatement Approach Procedures for the Sikorsky S-76," AHS Technical Specialists' Meeting for Rotorcraft Acoustics and Aerodynamics, October 1997.

[8]Gopalan, G., *Quasi-Static Acoustic Mapping of Helicopter Blade-Vortex Interaction Noise*, Ph.D. thesis, University of Maryland, 2004.

[9]Schmitz, F. H., Greenwood, E., Sickenberger, R. D., Gopalan, G., Sim, B. W.-C., Conner, D. A., Moralez, E., and Decker, W., "Measurement and Characterization of Helicopter Noise in Steady-State and Maneuvering Flight," American Helicopter Society 63rd Annual Forum, May 2007.

[10]Gopalan, G., Xue, M., Atkins, E., and Schmitz, F. H., "Longitudinal-Plane Simultaneous Non-Interfering Approach Trajectory Design for Noise Minimization," American Helicopter Society 59th Annual Forum, May 2003.

[11]Guntzer, F., Spiegel, P., and Lummer, M., "Genetic Optimizations of EC-135 Noise Abatement Flight Procedures using an Aeroacoustic Database," 35th European Rotorcraft Forum, September 2009.

[12]Morris, R., Johnson, M., Venable, K. B., and Lindsey, J., "Designing Noise-Minimal Rotorcraft Approach Trajectories," *ACM Trans. Intell. Syst. Technol.*, Vol. 7, (4), April 2016, pp. 58:1–58:25.

[13]Greenwood, E., Schmitz, F. H., and Gopalan, G., "Helicopter External Noise Radiation in Turning Flight: Theory and Experiment," American Helicopter Society 63rd Annual Forum, May 2007.

[14]Greenwood, E. and Schmitz, F. H., "A Parameter Identi-

fication Method for Helicopter Noise Source Identification and Physics-Based Semi-Empirical Modeling," American Helicopter Society 66th Annual Forum, May 2010.

[15]Greenwood, E., *Fundamental Rotorcraft Acoustic Modeling from Experiments (FRAME)*, Ph.D. thesis, University of Maryland, January 2011.

[16]Greenwood, E., Schmitz, F. H., and Sickenberger, R. D., "A Semiempirical Noise Modeling Method for Helicopter Maneuvering Flight Operations," *Journal of the American Helicopter Society*, Vol. 60, (2), 2015, pp. 1–13.

[17]Greenwood, E., Rau, R., May, B., and Hobbs, C., "A Maneuvering Flight Noise Model for Helicopter Mission Planning," American Helicopter Society 71st Annual Forum, May 2015.

[18]Sickenberger, R. D., *Modeling Helicopter Near-Horizon Harmonic Noise due to Transient Maneuvers*, Ph.D. thesis, University of Maryland, May 2013.

[19]Watts, M. E., Greenwood, E., Smith, C. D., Snider, R., and Conner, D. A., "Maneuver Acoustic Flight Test of the Bell 430 Helicopter Data Report," Technical Report TM2014-218266, NASA, 2014.

[20]Bass, H. E., Sutherland, L. C., Zuckerwar, A. J., Blackstock, D. T., and Hester, D. M., "Atmospheric absorption of sound: Further developments," *The Journal of the Acoustical Society of America*, Vol. 97, (1), 1995, pp. 680–683.

[21]Hargraves, C. R. and Paris, S. W., "Direct trajectory optimization using nonlinear programming and collocation," *Journal of Guidance, Control, and Dynamics*, Vol. 10, (4), 1987, pp. 338–342.

[22]Ingber, L., Petraglia, A., Petraglia, M. R., Machado, M. A. S., *et al.*, "Adaptive simulated annealing," *Stochastic global optimization and its applications with fuzzy adaptive simulated annealing*, Springer, 2012, pp. 33–62.

[23]Boggs, P. T. and Tolle, J. W., "Sequential quadratic programming," *Acta numerica*, Vol. 4, 1995, pp. 1–51.

[24]Cassis, J. H. and Schmit, L. A., "On implementation of the extended interior penalty function," *International Journal for Numerical Methods in Engineering*, Vol. 10, (1), 1976, pp. 1–23.

[25]Greenwood, E., Sim, B., and Boyd, D., "The Effects of Ambient Conditions on Helicopter Harmonic Noise Radiation," American Helicopter Society 72nd Annual Forum, May 2016.

[26]Watts, M., Greenwood, E., and Stephenson, J., "Measurement and Characterization of Helicopter Noise at Different Altitudes," American Helicopter Society 72nd Annual Forum, May 2016.

[27]Decker, W. A., Tucker, G. E., Moralez III, E., Hardy, G. H., and Lewis, E. K., "Use of a Portable Programmable Guidance Display in Support of Helicopter Noise Testing," American Helicopter Society 63rd Annual Forum, May 2007.